

# INTERCALATION OF METHYLENE BLUE INTO MONTMORILLONITE AT DIFFERENT CONDITIONS: AN APPROACH FOR PREPARING CLAY-BASED NANOPIGMENTS

#MAZDAK VALIDI, SAEED BAZGIR\*, ABOSAEED RASHIDI, MOHAMMAD ESMAIL YAZDANSHENAS\*\*

*Department of Textile Engineering, Science and Research Branch, Islamic Azad University, Tehran, Iran*

*\*Department of Polymer Engineering, Science and Research Branch, Islamic Azad University, Tehran, Iran*

*\*\*Department of Textile Engineering, Yazd Branch, Islamic Azad University, Yazd, Iran*

#E-mail: validi.m@srbiau.ac.ir

Submitted November 27, 2011; accepted February 10, 2012

**Keywords:** Montmorillonite, Intercalation, Cationic Exchange, Methylene blue, Nanopigment

*Intercalation products based on ionic exchange reaction between cationic dye methylene blue and Na<sup>+</sup>-montmorillonite were prepared. Montmorillonite particles intercalated with methylene blue were characterized using X-ray diffraction, infrared spectroscopy, elemental and thermo-gravimetric analysis. The results showed that intercalation of dye molecules within the interlayer spaces of montmorillonite has successfully occurred and a degree of layers coverage equal to 81 % of cationic exchange capacity was achieved. The obtained coverage results in an increase of 5.8 Å in the basal spacing of silicate layers compared to pure montmorillonite. XRD results also indicated that the intercalation process was only dependant on intercalant concentration. Other factors such as time of the process and clay concentration had no effect on the obtained basal spacing. Thermo-gravimetric analysis suggested improved thermal stability of the intercalated dye.*

## INTRODUCTION

Clay minerals can react with different types of organic compounds in particular ways [1]. Among them smectites, a group of 2:1-layer clay minerals, is highly reactive and has been known since 1940s to interact with organic molecules through electrostatic interactions (e.g. ion exchange), secondary bonding (e.g. adsorption of neutral species) or covalent bonding (e.g. grafting) to produce compounds that have found uses in a various industrial applications [2]. Montmorillonite which belongs to this group of layered silicates consists of thin platelets of less than 1 nm in thickness. Each platelet is comprised of aluminum octahedral layer which is linked to oxygen and is sandwiched between silicon tetrahedral layers. These layers are linked together by Van der Waals forces and are formed as stacks of plates. Each platelet has a large surface area and a high aspect ratio of over 200. A schematic structure of the MMT is shown in Figure 1. The charge of the aluminosilicate layer is negative which is neutralized by compensating exchangeable cations (e.g. Na<sup>+</sup>, Ca<sup>2+</sup>) and their coordinated water molecules in interlayer spaces. Smectites have attracted more attention because of its potential to be intercalated by various types of cationic organic molecules between the aluminosilicate layers by ion exchange process which introduces different applications for these host-guest systems [4, 5].

Hydrophobic or organophilic surface modification of clay mineral particles by electrostatic interaction of MMT with cationic surfactants, mainly quaternary alkylammonium compounds, have been widely practiced in the last decade [6]. The organoclays have superior compatibility with hydrocarbon molecules therefore, they have found important applications such as hydrocarbon removal or oil spill clean-up [7, 8] and polymer-clay nanocomposites [9].

Cationic dyes are another group of organic compounds which are used as an intercalant and their luminescence properties have been extensively investigated [5, 10]. The interaction of cationic dyes with clay mineral surfaces changes the spectroscopic properties of the dye molecules. Metachromasy caused by adsorption and aggregation of dye molecules on clay layers is one of the most studied photo-physical processes to probe the clay surface [11]. Progress in controlling photophysical and photochemical properties of clay-dye hybrids lead to production of advanced material [12-15]. Also MMT is considered as an efficient and low cost adsorbent for dye removal from colored wastewaters due to the high absorption capacity for cationic dye molecules [16, 17].

Using cationic dye intercalated MMT as colorant in coloration of polymeric matrices and printing inks are other new application of the MMT-dye hybrids [18, 19]. The main proposed aims of the new pigment, named "nanopigment", was to improve the UV stability of the

dye and to enhance mechanical properties by nano-scale dispersion of the colored silicate layers in polymer matrix [18]. In this area recently Raha et al. [20] reported that the color stability of the MMT/rhodamine B nanopigment in polypropylene was improved more than ten times compared with the pure dye due to the protection offered by the silicate layers to the intercalated dye molecules.

The objective of present paper was to attain an applicable method in preparation of a cationic dye intercalated montmorillonite suitable for polymer coloration. In this manner intercalation of methylene blue (MB) in montmorillonite (MMT) was done through an adsorption process in different conditions. Because of the importance of interlayer distance of prepared MB intercalated montmorillonite on the delamination and exfoliation processes in polymer, the variable factors were investigated based on the criterion. The intercalation quality of samples was assessed using X-ray diffraction technique. Moreover, infrared spectroscopy, CHN and TGA/DTG techniques were applied to further study thermal properties and elemental analysis of the intercalated products.

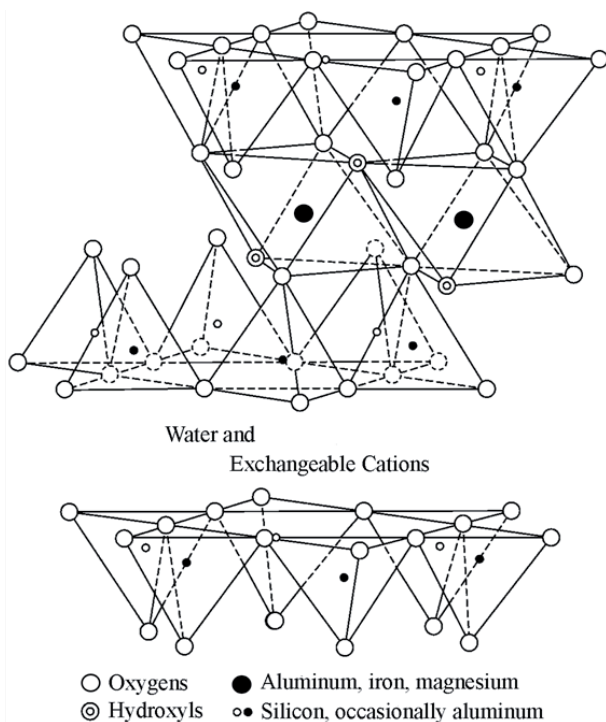


Figure 1. Molecular structure of montmorillonite, adopted from [3].

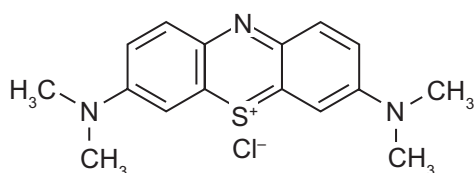


Figure 2. Molecular structure of the methylene blue.

## EXPERIMENTAL

### Materials

The clay fraction of bentonite which was composed of about 92% montmorillonite (MMT) was used to intercalate methylene blue in. The montmorillonite sample was prepared by subjecting the Na<sup>+</sup>-bentonite (originated from Ferdos Mine, Khorasan, Iran) suspension to repeated sedimentation until the <2 μm clay fractions were obtained. After drying, the sample was pulverized to pass through a 200 mesh sieve. Cation exchange capacity (CEC) of clay was determined by the ammonium acetate method [21] which was equal to 102 meq/100g.

Cationic dye, C.I. Basic blue 9 (52015), generally known as methylene Blue was purchased from Schawn (china). It was used without any further purification. The chemical structure of methylene blue is depicted in Figure 2.

### Preparation of methylene blue intercalated montmorillonite

Methylene blue intercalation into the montmorillonite was done at different conditions as quoted in Table 1. In each process, 1% wt. clay suspension was first

Table 1. Conditions of intercalation processes.

Sample code	Dye concentration (respect to the CEC of clay)	Intercalation time (hr)	Concentration of Clay suspension (wt. %)
MMT-MB (1)	0.5	3	1
MMT-MB (2)	1	3	1
MMT-MB (3)	1.2	3	1
MMT-MB (4)	1.3	3	1
MMT-MB (5)	1.3	3	3
MMT-MB (6)	1.3	12	1
MMT-MB (7)	1.5	3	1

prepared under mechanical stirring in deionized water for 3 hour. The pH of clay suspension and MB solution was adjusted to pH 9 and 5 respectively, using 0.1N HCl and NaOH. Then a pre-dissolved amount of dye ranging from 0.5 to 1.5 times of CEC of the montmorillonite (see Table 1) was slowly added to the clay suspension at room temperature and the reaction mixture was stirred for 3 hours. In preparation of two samples, MMT-MB (5) and MMT-MB (6), the methylene blue concentration was constant, equal to 1.3 times of CEC of clay. However concentration of clay suspension and the time of intercalation process were different. At the end of the process, the colored hybrid products were separated from liquid phase by centrifugation for 30 min at 4000 rpm. Then the separated phase was washed with deionized water repeatedly to remove any excess dye. After drying at room temperature, the intercalation products were ground using agate mortar and sieved through a 200 mesh sieve.

#### Characterization methods

##### *X-ray diffraction characterization*

X-ray diffraction (XRD) analysis of montmorillonite and MMT-MB samples was performed using a Bruker D8-ADVANCE X-ray powder diffractometer between 2 and 10° in steps of 0.02° with Cu K<sub>α</sub> radiation (30 mA, 40 kV).

##### *FTIR spectroscopy*

Infrared spectra of montmorillonite, MB and intercalated product were recorded using a Nicolet, Nexus 870 FTIR spectrophotometer by KBr pressed disk method. The spectra were collected for each measurement over the spectral range of 400-4000 cm<sup>-1</sup> with a resolution of 4 cm<sup>-1</sup>.

##### *Elemental analysis*

The percentage of carbon and nitrogen in montmorillonite and MMT-MB sample were determined using a 2400 Perkin-Elmer CHN Elemental Analyzer. The coverage of silicate layers of MMT by MB molecules or the amount of adsorbed MB molecules per 100g MMT-MB after intercalation process was determined using a method described by Dudkina et al. [22]. In first step the amounts of carbon and nitrogen per 100g of MMT-MB, n<sub>C</sub> and n<sub>N</sub> respectively, were calculated using Equation 1 based on the obtained carbon and nitrogen contents. In the formula X% is C or N content, M and M<sub>X</sub> are molar masses of MB molecule and X element respectively, and N<sub>X</sub> is number of X (carbon or nitrogen) atoms in MB molecule. The factor of 97.654 considers the Na content in 100 g MMT-MB sample.

$$n_x[\text{mmol}/100\text{g}] = \frac{97.654}{\frac{N_x \times M_x}{X[\text{wt\%}]/100} - M} \quad (1)$$

The degree of coverage is then calculated by dividing the average value of the n<sub>C</sub> and n<sub>N</sub> (in mmol/100 g) with respect to the CEC (102 mmol/100 g).

##### *Thermo gravimetric analysis*

Thermo gravimetric analysis (TGA) and its first derivative (DTG) experiments were carried out on montmorillonite, MB and MMT-MB sample using a Pyris Diamond (SII) Perkin Elmer Instruments. The samples (2-4 mg) were placed into alumina crucibles and scanned from 30°C to 800°C at a rate of 10°C/min in Nitrogen atmosphere in order to evaluate the thermal stability of the MB intercalated montmorillonite.

## RESULTS AND DISCUSSION

### XRD patterns of MB intercalated montmorillonites

Figure 3 shows the XRD patterns of MMT and the prepared MMT-MB samples with different concentration of MB. As it can be seen in the figure, the reflections of MMT-MB samples broadened and shifted to lower angles. The observed shift implied to the increase in the basal spacing from 12.56 Å for the untreated MMT to more expanded basal spacing which could be attributed to the intercalation of MB molecules into the interlayer spaces of montmorillonite. As the peaks suggest by increasing MB solution concentrations, the basal spacing would increase accordingly. Therefore, larger distances between the aluminosilicate layers were achieved in the intercalation processes with concentrated dye solutions. This trend was clearly presented in Figure 4 which shows the changes of MMT basal spacing up on increasing MB concentration. The results were in line with the study of Klika et al. [23]. Based on their report, highly concentrated solutions of MB contain higher agglomerates of MB which leads to higher MB cations content in the interlayer space. Consequently higher basal

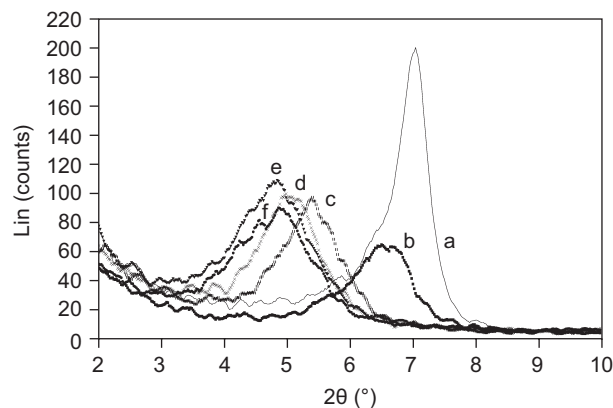


Figure 3. X-ray diffraction spectra of a) MMT, b) MMT-MB (1), c) MMT-MB (2), d) MMT-MB (3), e) MMT-MB(4), f) MMT-MB (7) samples.

spacing, especially for montmorillonites with higher layer charge density was achieved. The obtained results on the other hand imply that the adsorption capacity of MMT is higher than its CEC. In our adsorption isotherm study on MMT, equilibrium content of adsorbed MB of 625 mg/g which approximately equals to 1.65 times of CEC of MMT was obtained [24].

As it can be seen in Figure 3 and 4, obtained value for basal spacing of MMT-MB (7) sample (18.16 Å), was not significantly different from the MMT-MB (4) sample (18.3 Å). It indicates that the mentioned trend was leveled off when the value of the concentration of intercalant reached an amount equal to 1.3 times of CEC. So this concentration of MB was selected as an optimum level of intercalant concentration.

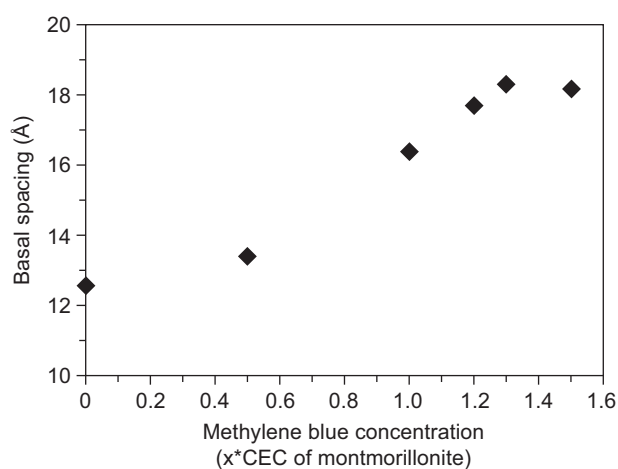


Figure 4. Effect of methylene blue concentration on basal spacing of intercalation products.

Based on the obtained basal spacing for MMT-MB (4) sample, we can conclude that the angle of the adsorbed dye to the silicate surface was significantly tilted and MB molecules are deposited in two layers. Similar results obtained in the work of Klika et al. [23] which maximum basal spacing around 18.6 Å experimentally and 18.4 up to 19 Å based on structure modeling was achieved. Recent works of Bujdák et al. [25] and Kaneko et al. [26] also showed that at higher basal spacing, which is the results of high layer charge of montmorillonite and more aggregated form of the dye, the orientation of intercalated dye molecules in the MMT interlayer become more tilted.

Table 2. Elemental analysis data of MMT and MMT-MB samples and calculated coverage percentage of the MMT layers by MB molecules.

Sample	C%	N%	H%	$n_C$ (mmol/100 g)	$n_N$ (mmol/100 g)	Coverage (mol %)*
MMT	0.22	0.03	1.35	–	–	–
MMT-MB (4)	12.42	2.9	1.82	79.65	86.54	81

\* Coverage with respect to the cation exchange capacity (CEC) of 102 meq/100 g

XRD spectra of three intercalated samples prepared with equal dye concentration, but in different concentration of clay suspension and time of intercalation process are presented in Figure 5. As it can be seen from the figure, there is no significant difference between these spectra and also their basal spacings. It implies that these two variables didn't have any effect on intercalation process in terms of interlayer spacing. Hence MMT-MB (4) sample was chosen for further characterizations.

It must be mentioned that broadening appeared in all of diffraction profiles, was arising from higher structural inhomogeneity. This confirms the saturation of MMT by more concentrated MB solutions and higher fractions of dye aggregates.

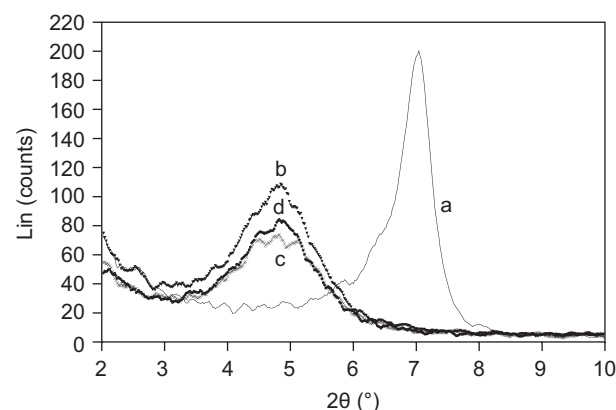


Figure 5. X-ray diffraction spectra of a) MMT, b) MMT-MB (4), c) MMT-MB (5), d) MMT-MB (6) samples.

#### CHN Analysis

The results of CHN elemental analysis of pure MMT and MMT-MB (4) sample are shown in Table 2. As expected the carbon content of MMT is negligible. However, it reached the amount of 12.42% in the MMT-MB sample, which indicates the existence of MB molecules in the layered structure of MMT. Since the MMT-MB samples was washed repeatedly to remove excess and loose bonded dye molecules, the majority of carbon content is attributed to intercalated molecules that bind to silicate layers mostly by stronger ionic bonding. The conclusions drawn from CHN data are supported by XRD measurements (see Figure 3), confirmed the intercalation of MB species in the interlayer spaces.

In order to quantify the amounts of MB in MMT-MB (4) sample, the coverage factor was calculated from the content of either C or N, according to Equation 1. The values are reported in Table 2. From the table, it could be seen that the amount of MB molecules equals to 81% of CEC of montmorillonite. This means that not all of added MB molecules to clay suspension bonded to silicate surfaces strongly and after removing loose and excess MB molecules, only a fraction of them can be intercalated by MMT layers. Similar results were obtained from coverage data corresponding to MMTs modified with hexadecyltrimethyl ammonium bromide in amount of two times of CEC, which coverage percentages of 115% based on this method was obtained [27].

#### FTIR spectroscopy

Infrared spectra of MMT, MB and MMT-MB are shown in Figure 6. As can be seen in the figure, the infrared curve of MMT showed characteristic smectitic clay mineral peaks. In this spectrum, strong band at  $1035.64\text{ cm}^{-1}$  was attributed to the Si-O stretching vibrations. The peak at  $1642.17\text{ cm}^{-1}$  and the broad band at  $3439.76\text{ cm}^{-1}$  were assigned to -O-H bending and stretching vibration modes of adsorbed water respectively [28, 29]. Also the peak at  $3629.83\text{ cm}^{-1}$  corresponds to the structural hydroxyl stretching vibration bonded to the aluminum and/or magnesium in montmorillonite. These peaks appeared in the spectrum of MMT-MB albeit of low intensity and small shift. The peak assigned to bending vibration mode of adsorbed water ( $3629.83\text{ cm}^{-1}$ ) disappeared in the spectrum of MMT-MB sample and the other one ( $3439.76\text{ cm}^{-1}$ ) was very weak. It seems that it was covered by MB band in this region. The intensities of bands around  $1600$  and  $3400\text{ cm}^{-1}$  are attributed to adsorbed water and/or hydration water, which decreased up on cationic exchange process with organic molecules [29].

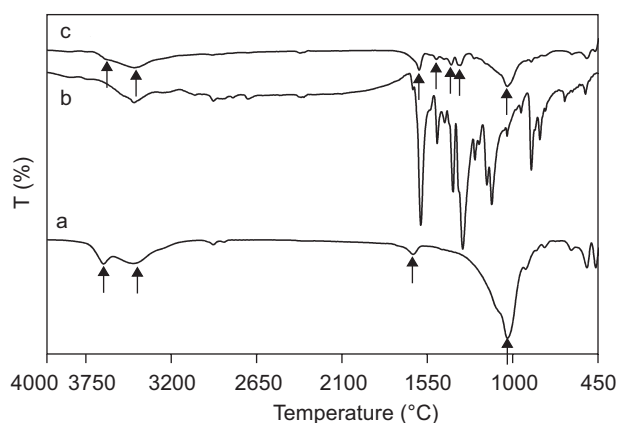


Figure 6. Infrared spectra of a) MMT, b) MB and c) MMT-MB (4) samples.

In spectrum of MB, the peaks at  $1591.50$  and  $1487.21\text{ cm}^{-1}$  were attributed to the stretching vibrations of C=C and C=N of aromatic rings in the polyheterocyclic molecule [30]. These bands with some small shifts were observed in the MMT-MB sample clearly at  $1491.91$  and  $1602.42\text{ cm}^{-1}$ . Similarly appeared band at  $1323\text{ cm}^{-1}$  in MB spectrum which were related to -C-N stretching of aromatic ring [31], shifted to higher wave numbers ( $1338.60\text{ cm}^{-1}$ ) due to the interaction with silicate layers in spectrum (c). The bands at  $2924.71$  and  $2865.63\text{ cm}^{-1}$  corresponded to asymmetric and symmetric vibration of C-H bonds in two  $\text{CH}_3$  groups. The peak that appeared at  $1385.62\text{ cm}^{-1}$  in MB spectrum attributed to the asymmetric  $\text{CH}_3$  bending vibration in dimethyl groups [32, 33]. It must be mentioned that the IR spectrum of MB at wave numbers higher than  $3100\text{ cm}^{-1}$  shows only a broad band between  $3400$  and  $3500\text{ cm}^{-1}$ , which could be due to the presence of a water molecule [34]. These peaks and other characteristic peaks of MB occurred in the MMT-MB spectrum with slight red shift which confirms the strong interaction of MB with silicate layers. This indicates the existence of MB as an intercalant in the exchanged products which is in connection with the results of CHN elemental analysis and XRD.

#### Thermogravimetric analysis

The results of thermo-gravimetric analysis of MMT, MB, and MMT-MB (4) samples are presented in Figure 7. The TGA data in the figure show that all samples had considerable amount of moisture as can be seen by drop in its mass below  $100^\circ\text{C}$ . As expected this initial step weight loss was more intense in the case of MMT. The DTG curves of MMT confirmed this idea clearly by drastic peak with maximum at  $65^\circ\text{C}$  (see Figure 8). The observed peak and the other at  $600-700^\circ\text{C}$  are due to the dehydration of adsorbed water molecules and dehydroxylation of silicate layers, respectively [28, 33]. As DTG curve of MMT-MB suggests, the first peak

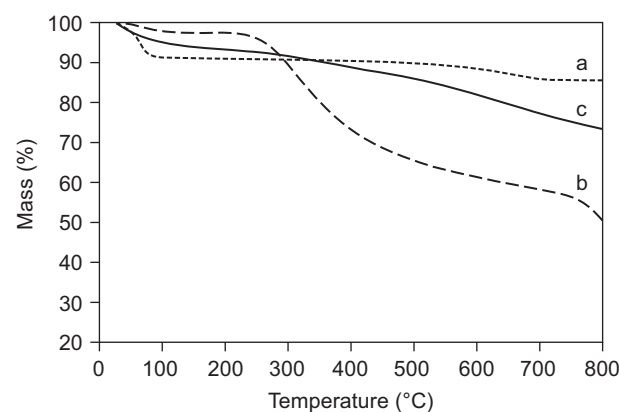


Figure 7. TGA curves for a) MMT, b) MB and c) MMT-MB (4) samples, measured at a heating rate of  $10^\circ\text{C}/\text{min}$  under  $\text{N}_2$  gas.

is weaker and broader. The presence of organic dye molecules on the clay surface makes it hydrophobic and consequently the peak maximum in the curve of organo-clay appears at a lower temperature compared to the untreated montmorillonite [35]. The DTG curves of both the montmorillonite and the dye, indicate that the moisture was almost totally removed at 100 and 120°C respectively, whereas for the MMT-MB sample the presence of moisture was observed at even higher temperatures of up to 150°C. This means that the water molecules were trapped within the MMT-MB structure due to constraint caused by intercalated MB molecules, which required a higher temperature to escape. Similar result about the dehydration peaks in the case of rhodamine B intercalated MMT [20].

Figure 8 shows that the onset of MB decomposition was occurred between 200 and 250°C. After passing this temperature a drastic weight loss about 45.6% was obtained. This decomposition step was clearly seen in DTG curve with an intense peak from 200 °C up to 500 °C. In the case of the MMT-MB sample, this trend was changed to a very slow and gradual rate of decomposition. The MB curve showed a sharp peak with a maximum at 309 °C, whereas in the DTG of the MMT-MB sample, only weak peak was observed with a maximum of 315 °C. In other words the onset of decomposition shifted to higher temperatures compared to pure MB. Considering the results of XRD, FTIR and CHN analysis, it is implied that the intercalation of MB molecules in interlayer spaces of MMT has occurred. Therefore, its thermal stability has improved accordingly.

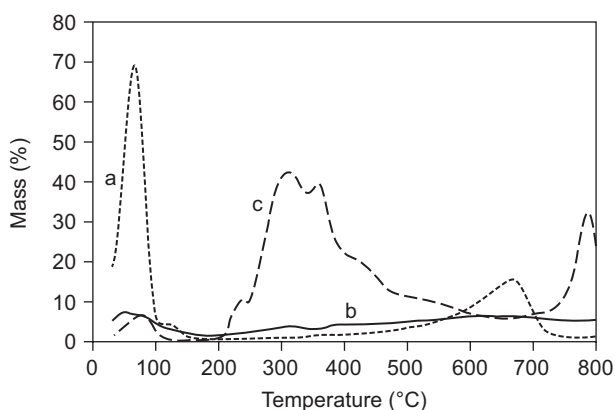


Figure 8. DTG curves for a) MMT, b) MB and c) MMT-MB (4) samples, measured at a heating rate of 10 °C/min under N<sub>2</sub> gas.

## CONCLUSION

The intercalation of montmorillonite with methylene blue cationic dye was performed in different conditions, in terms of MB & MMT concentration and process time. The results of XRD showed that the intercalation of MMT has successfully occurred and a basal spacing of 18.3 Å was obtained which corresponds to a bilayer

arrangement of MB molecules in montmorillonite interlayer, giving a thickness of about 5.8 Å. The results also indicated that interlayer space increased as the dye concentration escalated up to 1.3 times of CEC of montmorillonite. The intercalation process also was confirmed by the results of CHN and FTIR. TGA/DTG thermograms showed that the modification of MMT by MB decreases hydrophilicity of the surfaces of silicate layers. Also by the process, the thermal stability of MB molecules between interlayer of the layered silicate was increased in comparison to pure dye. By investigating some important parameters on intercalation of the MB in the clay layers, we have found a practical method to produce the intercalated product that can be used as a new colorant in melt processing (mass-pigmenting) of thermoplastic polymers. Its potential in coloration of polyolefines is our target for future work

## References

- Lagaly G., Ogawa M., Dekany I. in: *Handbook of clay science*, Ed. Bergaya F., Theng B.K.G., Lagaly G., p.309-379, Elsevier, Amsterdam 2006.
- Ruiz-Hitzky E., Aranda P., Serratos J.M. in: *Handbook of layered materials*, Ed. Auerbach S.M., Carrado K.A., Dutta P.K., p.91–154, Marcel Dekker, New York 2004.
- Murray H.H.: *Applied Clay Mineralogy, Occurrences, Processing and Application of Kaolins, Bentonites, Palygorskite- Sepiolite, and Common Clays*, 1<sup>st</sup> ed., p.12-13, Elsevier, Amsterdam 2007.
- Gomez-Romero P., Sanchez C.: *New J. Chem.* 29, 57 (2005).
- Schulz-Ekloff G., Wohrle D., Duffel B., Schoonheydt R. A.: *Microporous Mesoporous Mater.* 51, 91 (2002).
- Paiva L.B., Morales A.R., Diaz F.R.V.: *Appl. Clay Sci.* 42, 8 (2008).
- Lee S. Y., Kim S. J., Chung S. Y., Jeong C.H.: *Chemosphere* 55, 781 (2003).
- Carmody O., Frost R., Xi Y., Kokot S.: *J. Colloid Interface Sci.* 305, 17 (2007).
- Pavlidou S., Papaspyrides C. D.: *Prog Polym Sci* 33, 1119 (2008).
- Takagi S., Eguchi M., Tryk D. A., Inoue H.: *Langmuir* 22, 1406 (2006).
- Garfinkel-Shweky D., Yariv S.: *Clay Miner.* 34, 459 (1999).
- Ogawa M., Kuroda K.: *Chem. Rev.* 95, 399 (1995).
- Del Hoyo C., Vicente M.A., Rives V.: *Clay Miner.* 36, 541 (2001).
- Shinozaki R., Nakato T.: *Microporous Mesoporous Mater.* 113, 81 (2008).
- Ito K., Kuwabara M., Fukunishi K., Fujiwara Y.: *J. Imaging Sci. Technol.* 40, 275 (1996).
- Liu P., Zhang L.: *Sep. Purif. Technol.* 58, 32 (2007).
- Almeida C.A.P., Debacher N.A., Downs A.J., Cottet L., Mello C.A.D.: *J. Colloid Interface Sci.* 332, 46 (2009).
- Fischer H., Batenburg L.F.: US patent no. 6,648,959 (2003).
- Baez E., Quazi N., Ivanov I., Bhattacharya S.N.: *Adv. Powder Technol.* 20, 267 (2009).
- Raha S., Ivanov I., Quazi N.H., Bhattacharya S.N.: *Appl. Clay Sci.* 42, 661 (2009).

21. Rhoades J. D. in: *Methods of Soil Analysis, Part 2-Chemical and Microbiological Properties*, Ed. Page A. L., p.149–157, American Society of Agronomy / Soil Science Society of America, Madison- Wisconsin 1982.
  22. Dudkina M.M., Tenkovtsev A.V., Pospiech D., Jehnichen D., Hübler L., Leuteritz A.: *J. Polym. Sci.: Part B: Polym. Phys.* **43**, 2493 (2005).
  23. Klika Z., Čapková P., Horáková P., Valášková M., Malý P., Machán R., Pospíšil M.: *J. Colloid Interface Sci.* **311**, 14 (2007).
  24. Validi M., Bazgir S., Rashidi A., Yazdanshenas M.E.: *J. Textile Sci. Technol.* **5**, 75 (2010).
  25. Bujdák J., Iyi N., Kaneko Y., Sasi R.: *Clay Miner.* **38**, 561 (2003).
  26. Kaneko Y., Iyi N., Bujdák J., Sasi R., Fujita T.: *J. Colloid Interface Sci.* **269**, 22 (2004).
  27. Sharafi M., Validi M., Bazgir S., Gholami H. in: *Proc. 1<sup>st</sup> International Conference on Advances in Wastewater Treatment and Reuse*, p.218, University of Tehran, Tehran 2009.
  28. Kim N., Malhotra S. V., Xanthos M.: *Microporous Mesoporous Mater.* **96**, 29 (2006).
  29. Zhou Q., Frost R. L., He H., Xi Y., Liu H.: *J. Colloid Interface Sci.* **307**, 357 (2007).
  30. Pavia D. L., Lampman G. M., Kriz G. S., Vyvyan J. R.: *Introduction to Spectroscopy*, 4<sup>th</sup> ed., p.15-104, Brooks / Cole, Cengage Learning, California 2009.
  31. Imamura K., Ikeda E., Nagayasu T., Sakiyama T., Nakanishi K.: *J. Colloid Interface Sci.* **245**, 50 (2002).
  32. Chen C., Mu S.: *J. Appl. Polym. Sci.* **88**, 1218 (2003).
  33. Shen W., He H., Zhu J., Yuana P., Frost R. L.: *J. Colloid Interface Sci.* **313**, 268 (2007).
  34. Shan D., Mu S.: *Chin. J. Polym. Sci.* **19**, 359 (2001).
  35. Yariv S. in: *Thermal analysis in the geoscience*, p.328-352, Ed. Smykatz-Kloss W., Warne S.J., Springer, Berlin 1991.
-